Top Catal (2014) 57:1372–1376
DOI 10.1007/s11244-014-0305-5

Catalytic Hydrocarbon Oxidation by Palladium-bis-NHC-Complexes

Dominik Munz · Thomas Strassner

Published online: 4 September 2014

Abstract We report density functional theory studies on the CH-activation and functionalization of methane and propane by palladium (II) complexes with chelating bis(NHC) ligands. The combined experimental and computational results indicate that a palladium tetrahalogenido complex is the resting state of the reaction, while the CH-activation constitutes the rate-determining step of the catalytic cycle.

Keywords CH activation · NHC · Palladium · DFT · Methane

1 Introduction

Natural gas and lower hydrocarbons constitute a vast fossil feedstock and energy resource. Direct petrochemical conversion of lower alkanes to liquid products like alcohols would open up new possibilities for the chemical industry and promises the reduction of CO_2 emissions [1, 2]. Therefore, the development of low-temperature, selective C–H activation protocols is highly desirable. The selective functionalization of lower alkanes and especially methane remains a challenge, despite of significant scientific progress during the last decades [1, 3–7]. Approaches relying on transition metals have received a lot of attention since the seminal work of Shilov in the early 1970s [2, 8, 9], however the implementation of a highly selective catalytic process remains to be accomplished.

Many of the reported catalytic C–H activation methods only work under strongly acidic conditions using expensive oxidants. Hence, the biggest challenges for the development of an economically viable process are the development of efficient co-oxidation protocols relying on molecular oxygen [10–12] and the substitution of aggressive acidic solvents by environmentally benign solvents.

More than a decade ago our group contributed the catalytic activation and efficient functionalization of methane by palladium(II) complexes with chelating bis-*N*-heterocyclic carbene (NHC) ligands in trifluoroacetic acid (HOTFA) [13]. These chelating bis-NHC ligands lead to superior reactivity and catalyst stability compared to other reports on palladium(II) catalysis without NHC ligands [7, 14, 15]. Later we examined the influence of the bis-NHC ligand design and transition metal [16–19], determined counterion effects [20], and extended our studies to propane [18, 21]. In the reaction with propane, we experimentally observed the predominant formation of *iso*-propyl trifluoroacetate (Fig. 1).

As density functional theory (DFT) calculations have proven to be a valuable tool for the investigation of CH activation mechanisms [22–27], we decided to model the mechanism of the palladium-bis(NHC) complex catalyzed CH functionalization of methane [28]. We proposed, based on previous work and the synthesis and reactivity of potential intermediates (Fig. 2) [29–35] that the reaction proceeds through a palladium catalyst in the oxidation states of +II and +IV and that the oxidation step is mediated by bromine. The C–H activation step was predicted to be the rate determining state of the catalytic cycle with an overall barrier of $\Delta G^{\neq} = +39.5$ kcal mol^{-1}.

Furthermore, the calculations predicted that the C–H activation by **2** is preceded by an oxidative exchange of the

Electronic supplementary material The online version of this article (doi:10.1007/s11244-014-0305-5) contains supplementary material, which is available to authorized users.

D. Munz · T. Strassner (✉)
Department of Chemistry and Food Chemistry, Technical University Dresden, Bergstrasse 66, 01069 Dresden, Germany
e-mail: thomas.strassner@chemie.tu-dresden.de

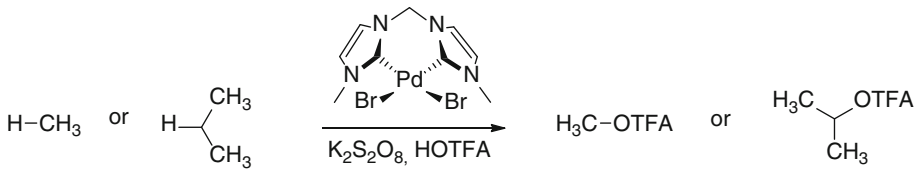

Fig. 1 Functionalization of methane or propane in trifluoroacetic acid

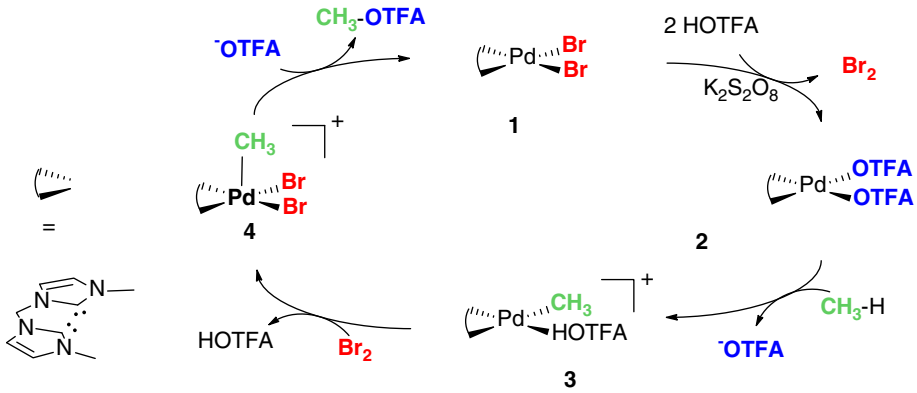

Fig. 2 Proposed catalytic cycle

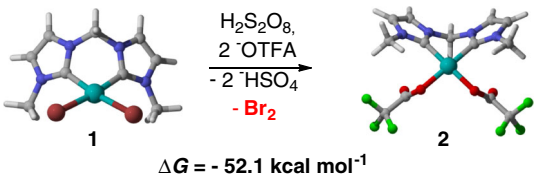

Fig. 3 Oxidative exchange of bromido ligands

bromido for the trifluoroacetato ligands by persulfate (Fig. 3).

Herein, we present further DFT calculations on the mechanism of the alkane oxidation by palladium(II) catalysts with chelating bis(NHC) ligands. We report additional information on the mechanism, the resting state of the overall mechanism, and the rate determining step for the activation of propane as well.

2 Computational Details

The calculations were performed with Gaussian03 [28, 36] as previously described in detail [28, 36]. The DFT hybrid model B3LYP [37–40] was used together with the 6-31G(d) basis set [41–43] for geometry optimizations, palladium was described using a decontracted Hay-Wadt(n + 1) ECP and basis set [44]. No symmetry or internal coordinate constraints were applied during optimizations. All reported intermediates were verified as true minima by the absence of negative eigenvalues in the vibrational frequency analysis. Transition state structures (indicated by ts) were located using the Berny algorithm until the Hessian matrix had only one imaginary eigenvalue. The identity of all transition states was confirmed by animating the negative eigenvector coordinate with MOLDEN [45] and by an intrinsic reaction coordinate calculation. The energies of reactants, products and transition states have been corrected by triple-ζ single-point calculations on the 6-311 ++G(d,p) level of theory [46–48], CPCM solvent calculations on the optimized geometries [49, 50], and by applying the dispersion correction DFT-D3 V2.1, Rev. 6 [51] with BJ damping [52] and $s_6 = 1.0$. It has been reported that the inclusion of dispersion effects significantly improves the performance of the B3LYP functional in the treatment of metal-alkane interactions [53]. The CPCM solvent parameters were selected for trifluoroacetic acid (experimentally determined dielectric constant: 8.55 [54]) with an experimental density derived solvent probe radius of 2.479 Å, using UAKS radii for the solute atoms. For acetic acid the experimentally determined dielectric constant of 6.60 [55] has been used.

All energies reported are Gibbs free energies at standard conditions ($T = 298$ K, $p = 1$ atm) using unscaled frequencies. Approximate Gibbs free energies were obtained through thermochemical analysis, using the thermal correction to the Gibbs free energy as reported by Gaussian03 (including zero point effects, thermal enthalpy corrections and entropy) and additionally taking into account the D3 correction and dispersion, repulsion and cavitation energy corrections of the CPCM solvent model. This procedure has been recommended for the calculation of transition metal complexes [56]. Electronic energies including dispersion and solvent effects are given in the Supporting Information. The Hessian matrix required for vibrational analysis was calculated on the double-ζ level of theory.

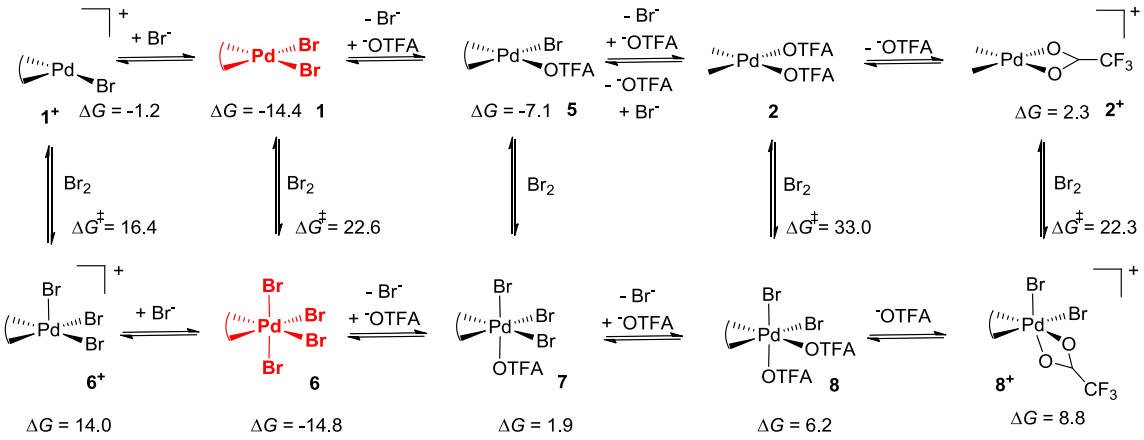

Fig. 4 Coordination and ligand exchange phenomena. Values are given in kcal mol^{-1} relative to compound **2**

The trifluoroacetate and the bromide anions have been treated by explicit solvation. The energies of those clusters converged nicely within four coordinating solvent molecules. In cases where different isomers could be formed, all isomers have been calculated, but only the most stable one is shown.

3 Results and Discussion

Our computational results [28] predict that the trifluoroacetate complex **1_(OTFA)$_2$** (cf. Figure 2) should be the resting state of the mechanism. Unfortunately, we could not unambiguously verify the presence of **1_(OTFA)$_2$** in the reaction mixture by ^{1}H NMR. This is due to the fact that anions (e.g. halides) present in the reaction mixture interact with the "acidic" CH_2 bridge of the chelating ligand; for relevant ^{1}H NMR spectra and a thorough discussion please see the Supplementary Material and Ref. [32]. Nevertheless, the observation of a red-brown colored precipitate during the catalysis points toward the formation of palladium(IV) species. In addition the formation of palladium(IV) species after the addition of persulfate to **1_Br$_2$** in HOTFA (and heating over night at 60 °C) was proven by ^{1}H NMR spectroscopy. For experimental details and the relevant ^{1}H NMR spectra, please see the Supplementary Material. In order to further explore the nature of the resting state, we consequently calculated potential coordination pre-equilibria prior to the formation of the catalytically potent intermediate **1_(OTFA)$_2$**. Figure 4 shows the most stable potential intermediates.

The calculations predict that under non-oxidative conditions the palladium(II) complex **1** with two coordinating bromido ligands is the most stable compound ($\Delta G = -14.4$ kcal mol^{-1}). Nevertheless, the endergonic interconversion to the trifluoroacetate coordinating compound **2** via intermediate **5** ($\Delta G = -7.1$ kcal mol^{-1}) should be thermodynamically feasible under the reaction conditions employed ($T = 90$ °C). Likewise, **1** and **2** are predicted to stand in equilibrium with their positively charged species **1$^+$** and **2$^+$** (**1$^+$**: $\Delta G = -1.2$ kcal mol^{-1}, **2$^+$**: $\Delta G = +2.3$ kcal mol^{-1}).

However, our experimental observations (*e.g.* the presence of bromine) are consistent with the prediction that under oxidative conditions the palladium(IV) compound **6** with four coordinating bromido ligands will become the global minimum (**6**: $\Delta G = -14.8$ kcal mol^{-1})!

As compound **6** is not soluble in trifluoroacetic acid [32], our calculations even underestimate the preference for the formation of **6**. Comparable to the case of palladium(II), also the palladium(IV) complex is predicted to undergo endergonic ligand exchange reactions with the solvent to form the complexes **7** ($\Delta G = +1.9$ kcal mol^{-1}) and **8** ($\Delta G = +6.2$ kcal mol^{-1}). The positively charged species **6$^+$** ($\Delta G = +14.0$ kcal mol^{-1}) and **8$^+$** ($\Delta G = +8.8$ kcal mol^{-1}) are predicted to be viable intermediates under these reaction conditions as well. We also looked at the transition states for the oxidative addition of Br_2 in order to check for the kinetic barriers for the formation of the palladium(IV) complexes. As expected, all transition states lie well below ($\Delta G^{\neq} = 16.4$ kcal mol^{-1}, 22.6 kcal mol^{-1}, 33.9 kcal mol^{-1}, 22.3 kcal mol^{-1}) the overall reaction barrier we modeled [28] for the whole catalytic cycle ($\Delta G^{\neq} = 39.5$ kcal mol^{-1}). In conclusion, our calculations are in agreement with our experimental observations of the formation of the palladium(IV) compound **6**, which also corresponds to the resting state of the catalytic cycle. Together with the formation of compound **6** under oxidative conditions by removal of bromide from the solution according to Fig. 5, two complexes **5** with one trifluoroacetato and one bromido ligand each are formed.

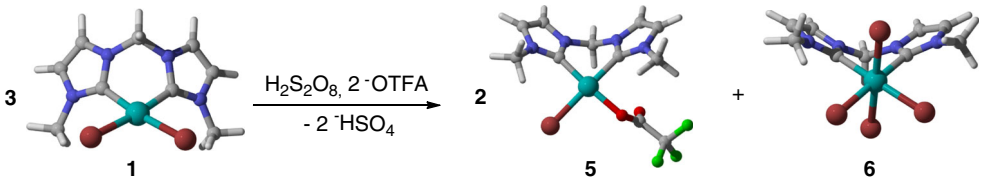

Fig. 5 Oxidative formation of complexes **5** and **6**

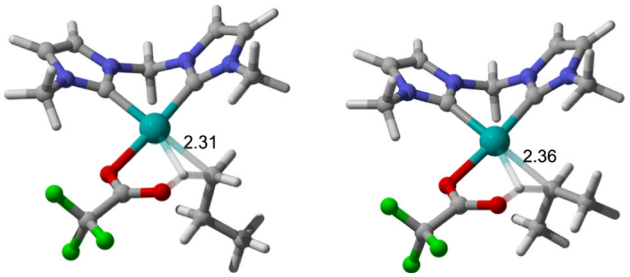

$^{n\text{Pr}}$**ts[2$^+$>3]** $^{i\text{Pr}}$**ts[2$^+$>3]**

$\Delta G^{\neq}$ = +38.1 kcal mol^{-1} $\Delta G^{\neq}$ = +43.1 kcal mol^{-1}

Fig. 6 Transition states for the activation of propane

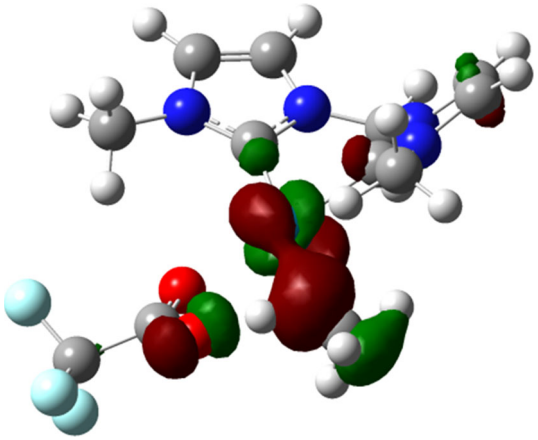

Fig. 7 Isodensity plot (0.06 a.u.) of the HOMO in the transition state **ts[2$^+$>3]** for methane

We then also investigated the activation of propane. The main difference between the activation of the C_1 substrate methane and the C_3 substrate propane is the regiochemistry between the *n*- and the *iso*-position. We therefore calculated the rate determining transition states for both pathways, the activation at the *iso*- and *n*-position of propane (Fig. 6).

The DFT results clearly indicate a preference for the activation of the terminal CH_3 instead of the internal CH_2 group ($\Delta\Delta G^{\neq} = +5.0$ kcal mol^{-1}). The transition state for the activation of the terminal methyl group of propane is also 1.4 kcal mol^{-1} more favorable than the transition state for the activation of methane ($\Delta G^{\neq} = +39.5$ kcal mol^{-1}). This is in nice agreement to the observation that the functionalization of propane proceeds at temperature about 20 °C lower compared to methane. The transition state for the C–H activation can be understood as the nucleophilic interaction [25] of the two electrons of the σ-C–H bond of the alkane with a d-orbital of the transition metal (Fig. 7). The interaction in the HOMO of **ts[2$^+$>3]** can also be rationalized in terms of the transient formation of a 3-center-2-electron bond situation between the palladium atom, the transferred proton, and the carbon atom of the alkane.

Contrary to the predictions by DFT, we experimentally observe the formation of about 90 % of *iso*-propyl trifluoroacetate and only about 5 % *n*-propyl trifluoroacetate. We therefore conclude, that in case of propane either the CH activation step is followed by an isomerization step as has been reported in the case of cobalt catalysis [57], or that another mechanism than in the case of methane is operating. Potential alternative mechanisms of CH functionalization include radical reactivity due to the formation of bromine in the reaction mixture, or the formation of electrophilic Br^+ species in the presence of Lewis acids [58–60]. Mechanistic studies (experiment and DFT) in order to clarify the reaction mechanism for propane are underway in our laboratories and will be reported in due course.

4 Conclusions

In conclusion, we present a DFT study on the functionalization of methane and propane by palladium complexes with bis(NHC) ligands. Coordination phenomena of the catalyst have been investigated and the calculations predict that the resting state of the reaction is a tetrahalogenido palladium(IV) complex. This result is in agreement with experimental observations. In the reaction with propane the calculation of the rate determining transition state indicates that the formation of *n*-propyl trifluoroacetate should be preferred, whereas experimentally the predominant formation of *iso*-propyl trifluoroacetate is observed. Further work therefore aims at rationalizing the discrepancy between the computational and the experimental results.

5 Supplementary Material

The complete Gaussian citation [36] and ^{1}H-NMR spectra showing the formation of palladium(IV) species after the addition of persulfate to complex **1** in HOTFA and experimental details thereof.

Acknowledgments The authors thank the center for Information Services and High Performance Computing (ZIH) for computation time and the Deutsche Forschungsgesellschaft DFG (STR 526/7-1 and STR 526/7-2) for financial support. D. M. also thanks the Studienstiftung des Deutschen Volkes. Donations of trifluoroacetic acid by Solvay Fluor are gratefully acknowledged.

References

1. Webb JR, Bolaño T, Gunnoe TB (2011) ChemSusChem 4:37
2. Shilov AE, Shulpin GB (2002) Activation and catalytic reactions of saturated hydrocarbons in the presence of metal complexes. Kluwer Academic New York, Boston
3. Chepaikin EG (2011) Russ Chem Rev 80:363
4. Labinger JA, Bercaw JE (2002) Nature 417:507
5. Schwarz H (2011) Angew Chem Int Ed 50:10096
6. Hashiguchi BG, Bischof SM, Konnick MM, Periana RA (2012) Acc Chem Res 45:885
7. Sen A (1998) Acc Chem Res 31:550
8. Gol'dshleger NF, Es'kova VV, Shilov AE, Shteinman AA, Fiz Zh (1972) Khim 46:1353
9. Gol'dshleger NF, Tyabin MB, Shilov AE, Shteinman AA, Fiz Zh (1969) Khim 43:2174
10. Vedernikov AN (2012) Acc Chem Res 45:803
11. Campbell AN, Stahl SS (2012) Acc Chem Res 45:851
12. Boisvert L, Goldberg KI (2011) Acc Chem Res 45:899
13. Muehlhofer M, Strassner T, Herrmann WA (2002) Angew Chem Int Ed 41:1745
14. Gol'dshleger NF, Moravskii AP (1994) Russ Chem Rev 63:125
15. Jia C, Kitamura T, Fujiwara Y (2001) Acc Chem Res 34:633
16. Ahrens S, Zeller A, Taige M, Strassner T (2006) Organometallics 25:5409
17. Meyer D, Taige MA, Zeller A, Hohlfeld K, Ahrens S, Strassner T (2009) Organometallics 28:2142
18. Munz D, Poethig A, Tronnier A, Strassner T (2013) Dalton Trans 42:7297
19. Ahrens S, Strassner T (2006) Inorg Chim Acta 359:4789
20. Strassner T, Muehlhofer M, Zeller A, Herdtweck E, Herrmann WA (2004) J Organomet Chem 689:1418
21. Munz D, Strassner T (2014) Angew Chem Int Ed 53:2485
22. Balcells D, Clot E, Eisenstein O (2010) Chem Rev 110:749
23. Boutadla Y, Davies DL, Macgregor SA, Poblador-Bahamonde AI (2009) Dalton Trans 30:5820
24. Figg TM, Webb JR, Cundari TR, Gunnoe TB (2012) J Am Chem Soc 134:2332
25. Ess DH, Goddard WA, Periana RA (2010) Organometallics 29:6459
26. Cundari TR, Prince BM (2011) J Organomet Chem 696:3982
27. Harvey JN (2001) Organometallics 20:4887
28. Munz D, Meyer D, Strassner T (2013) Organometallics 32:3469
29. Meyer D (2011) Azoliumsalze als NHC-Precursoren für Katalysatoren (Pd, Pt) zur Methanaktivierung sowie als ionische Flüssigkeiten—Synthese, DFT-Rechnungen und mechanistische Studien, Doctoral Thesis, TU Dresden, Dresden, Germany
30. Meyer D, Ahrens S, Strassner T (2010) Organometallics 29:3392
31. McCall AS, Kraft S (2012) Organometallics 31:3527
32. McCall AS, Wang H, Desper JM, Kraft S (2011) J Am Chem Soc 133:1832
33. Subramanium SS, Slaughter LM (2009) Dalton Trans 9:6930
34. Sluijter SN, Warsink S, Lutz M, Elsevier CJ (2013) Dalton Trans 42:7365
35. Finger M (2008) Synthese neuer elektronenreicher kationischer Palladium- und Platinkomplexe und ihr Verhalten in Carbonylierungsreaktionen, Doctoral Thesis, Unviersität Heidelberg, Heidelberg, Germany
36. Frisch MJ et al (2003) Gaussian 03, Rev. E.01. Gaussian, Inc, Pittsburgh
37. Becke AD (1993) J Chem Phys 98:5648
38. Lee C, Yang W, Parr RG (1988) Phys Rev B 37:785
39. Stephens PJ, Devlin FJ, Chabalowski CF, Frisch MJ (1994) J Phys Chem 98:11623
40. Vosko SH, Wilk L, Nusair M (1980) Can J Phys 58:1200
41. Hehre WJ, Ditchfield R, Pople JA (1980) J Chem Phys 56:2257
42. Francl MM, Pietro WJ, Hehre WJ, Binkley JS, Gordon MS, DeFrees DJ, Pople JA (1982) J Chem Phys 77:3654
43. Binning RC Jr, Curtiss LA (1990) J Comput Chem 11:1206
44. Wadt WR, Hay PJ (1985) J Phys Chem 82:299
45. Schaftenaar G, Noordik JH (2000) J Comput-Aided Mol Des 14:123
46. McLean AD, Chandler GS (1980) J Chem Phys 72:5639
47. Krishnan R, Binkley JS, Seeger R, Pople JA (1980) J Chem Phys 72:650
48. Curtiss LA, McGrath MP, Blaudeau JP, Davis NE, Binning RC, Radom L (1995) J Chem Phys 103:6104
49. Barone V, Cossi M (1998) J Phys Chem A 102:1995
50. Cossi M, Rega N, Scalmani G, Barone V (2003) J Comp Chem 24:669
51. Grimme S, Antony J, Ehrlich S, Krieg H (2010) J Chem Phys 132:154104
52. Grimme S, Ehrlich S, Goerigk L (2011) J Comput Chem 32:1456
53. Flener-Lovitt C, Woon DE, Dunning TH, Girolami GS (2010) J Phys Chem A 114:1843
54. Harris FE, Okonski CT (1954) J Am Chem Soc 76:4317
55. De Vrieze S, Westbroek P, Van Camp T, De Clerck K (2010) J Appl Polym Sci 115:837
56. Ryde U, Mata RA, Grimme S (2011) Dalton Trans 40:11176
57. Stolarov IP, Vargaftik MN, Shishkin DI, Moiseev II (1991) J Chem Soc Chem Commun 14:938
58. Olah GA, Prakash GKS (2006) Electrophilic Reactions of Alkanes. The Chemistry of Alkanes and Cycloalkanes. John Wiley & Sons Ltd, Chichester
59. Fokin AA, Schreiner PR (2002) Chem Rev 102:1551
60. Akhrem I, Orlinkov A (2007) Chem Rev 107:2037